Finite element simulation of the intramyocardial coronary circulation

FINITE ELEMENT SIMULATION OF THE INTRAMYOCARDIAL CORONARY CIRCULATION

Jacques M. Huyghe*, Cees W. Oomens°, Dick H. van Campen°, Theo Arts*, R.M. Heethaar+

* Dept. of Biophysics, Univ. of Limburg, Maastricht, The Netherlands
° Dept. of Mech. eng., Eindhoven Univ. of Techn., Eindhoven, The Netherlands
+ Dept of Biomed. Eng, Twente Univ., Enschede, The Netherlands

Abstract

A series of two axisymmetric finite element models of left ventricular mechanics is presented: a deformation model and a perfusion model. The deformation model computes variations of stress, strain and intramyocardial pressure during the cardiac cycle. The intramyocardial pressure field computed by the deformation model is substituted as an extravascular pressure in a coronary perfusion model. Computed strain, pressure and flow are compared with experimental data from the literature.

Introduction

Many authors illustrated the capabilities of the finite element method for stress and strain analysis of the myocardial wall. The method can also be used to simulate the coronary circulation.

The deformation model

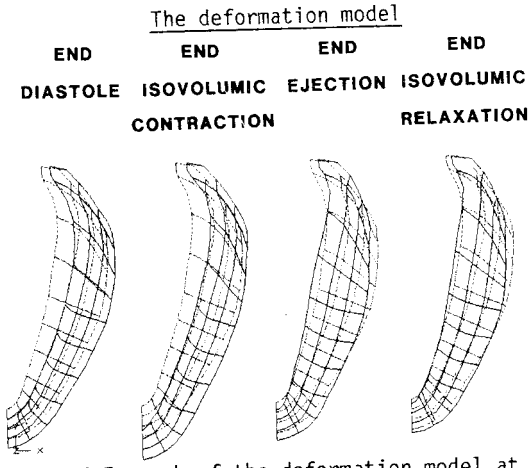

Fig. 1. F.E.-mesh of the deformation model at four different times during the cardiac cycle (continuous line), and in the reference state (dotted line).

30 8-node two-phase axisymmetric finite elements are used to represent the left ventricular wall. The geometry is derived from multiplanar X-ray tomographic data supplied by the biodynamics group of the Mayo clinic, Rochester, Minnesota. A continuous fiber angle distribution across the wall is chosen according to Streeter et al.[1]. A radial, axial and circumferential displacement is computed

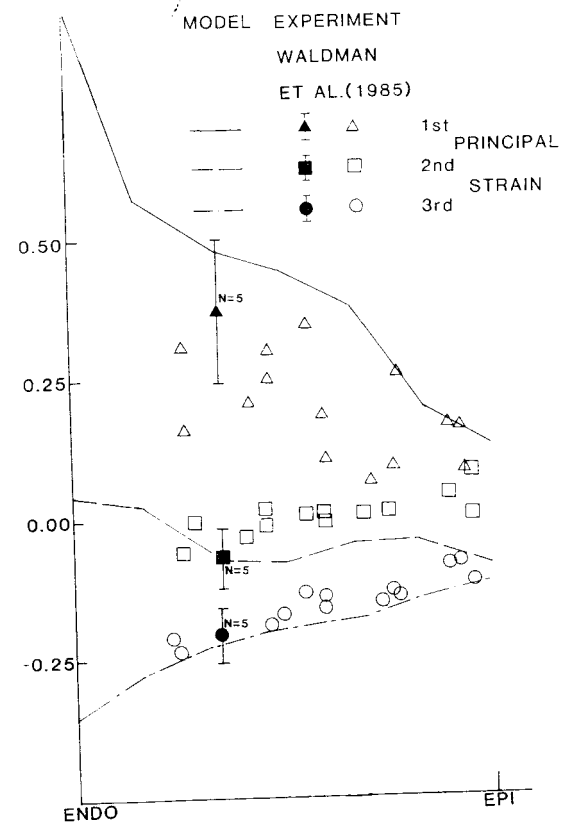

Fig. 2. Transmural course of principal finite strains at the equator.

for each of the 117 nodes. The circumferential displacement allows the ventricle to twist about its symmetry axis. For the corner nodes we compute in addition the local intramyocardial pressure. The tissue is modelled as a spongy material (= two-phase material) saturated with coronary blood: redistribution of coronary blood within the wall is possible. Exchange of blood between the intramyocardial coronary bed and the large epicardial coronary vessels is possible as well. No blood is allowed to cross the endocardial surface. No distinction is made between the different microvascu-

0276-6574/88/0000/0335$01.00 © 1988 IEEE

lar compartments, nor between intravascular and extravascular space. The passive properties of the myocardial tissue are described by an orthotropic quasi-linear viscoelastic law. The parameters of the law are derived from experimental data of several authors[2,3,4]. A time, strain and strain rate dependent contractile fiber stress is superimposed on the passive stress during the systolic phase. The downstream boundary condition is described by a linear 4 element model of the peripheral circulation borrowed from Westerhof et al.[5]. Transmural equatorial distribution of strain and intramyocardial pressure are consistent with experimental data from the literature[6,7,8,9] (fig. 2).

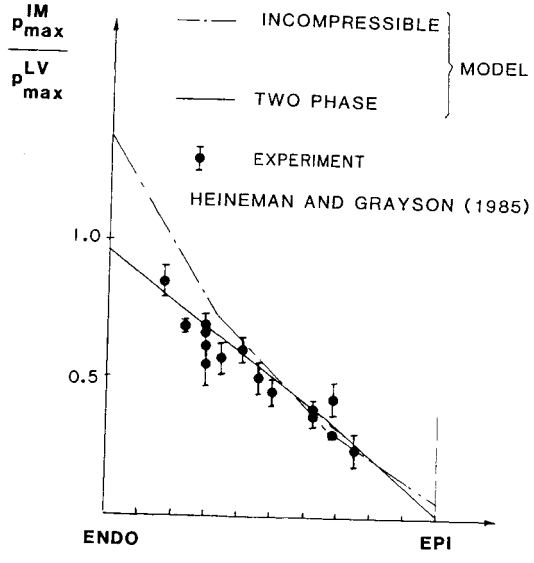

Fig. 3. Transmural equatorial distribution of intramyocardial pressure.

When the model is assigned a spongy nature (two-phase behaviour), the subendocardial tissue pressure is almost equal to the intraventricular pressure (fig. 3). However, when the material properties are switched to incompressibility (no redistribution of coronary blood within the wall), the subendocardial tissue pressure is found to exceed intraventricular pressure significantly. This result suggests that intracoronary blood may play an important role in reducing subendocardial tissue pressure in the in vivo ventricle. Finally when the model undergoes a systolic contraction without generating pressure in the intraventricular cavity, the systolic subendocardial tissue pressure is about as high as in a normal cardiac cycle whether the ventricle is modelled as a two-phase material (fig. 4) or as an incompressible material.

Perfusion model

The perfusion model is an axisymmetric version of the finite element model discussed in the companion paper. The finite element mesh is obtained by

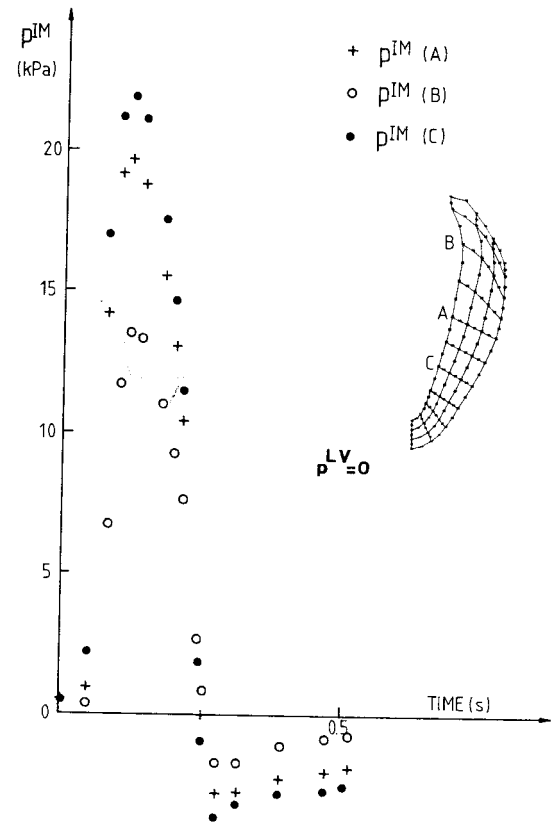

Fig. 4. Model result of subendocardial intramyocardial pressure during a left ventricular contraction at $p^{LV}=0$ (two-phase simulation).

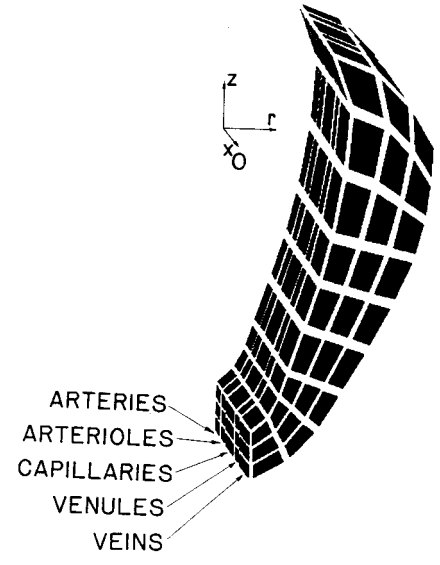

Fig. 5. The finite element mesh of the perfusion model.

extending the mesh of fig. 1 in a hyperdimension (fig. 5). Each layer of 27 elements represents one microvascular compartment. The conductance parameters of each compartment are evaluated on the basis of qualitative anatomical data of the geometry of the coronary tree and experimental data from the literature of intracoronary blood pressures and flow. Non-linear elastic properties are attributed to the vessel walls (fig. 6). The intramyocardial pressure field computed by the deformation model is substituted as an extravascular pressure. At the epicardial surface arterial coronary pressure is set to 11 kPa and venous coronary pressure is set to 0.5 kPa. The coronary pressure is computed every 5 ms for every node. High systolic endocardial coronary pressures are computed for all the compartments, while during diastole most of the coronary pressure drop occurs in the arterioles (fig. 7).

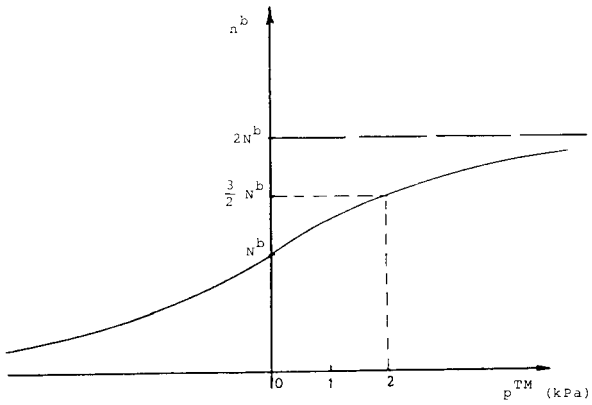

Fig. 6. Non-linear compliance of the microcirculatory compartments. n^b: current blood volume per unit arteriovenous parameter, N^b: initial blood volume per unit arteriovenous parameter, p^{TM}: transmural pressure drop across the vessel wall. The value of N^b is different for each finite element layer and is chosen according to Spaan[10].

The high systolic transmural pressure gradient results in a significant reduction of arterial coronary flow and a significant increase of venous coronary flow during systole (fig. 8). These strong alteration of coronary flow during systolic contraction are predicted by the model not only for the normal cardiac cycle but also during contraction of an unloaded ventricle (left ventricular pressure = 0). The poor sensitivity of the systolic reduction of arterial coronary flow to the systolic intraventricular pressure is consistent with unpublished experimental data of R. Krams and N. Westerhof (Free university, Amsterdam).

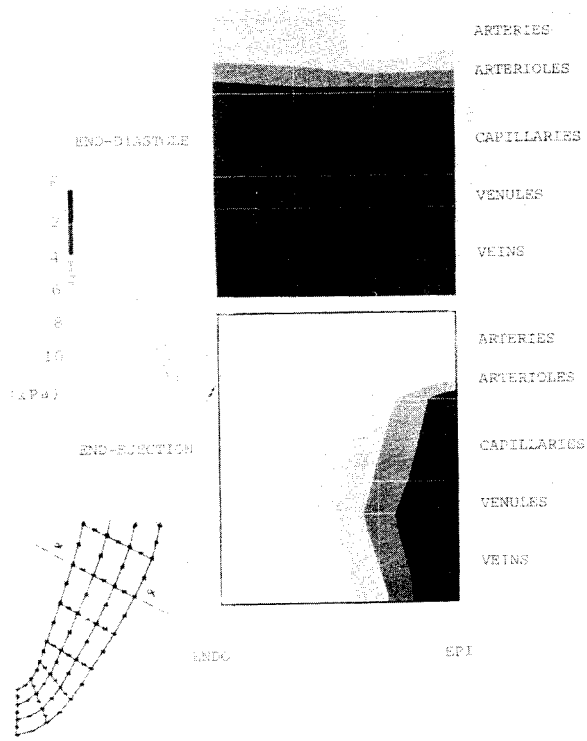

Fig. 7. Transmural coronary blood pressure distribution in section α-α of the left ventricular model.

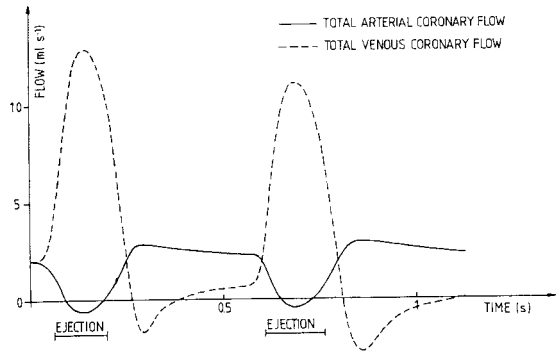

Fig. 8. Total coronary flow as predicted by the perfusion model.

Fig. 9 shows the arterial coronary flow pattern at end-diastole for the normal cardiac cycle and after occlusion. The top panel pertains to the basal condition: arterial blood flows then from the epicardial surface into the wall. The bottom panel pertains to the situation after occlusion. In this case significant collateral flow is predicted along the epicardial plexus from the healthy muscle to the ischaemic muscle.

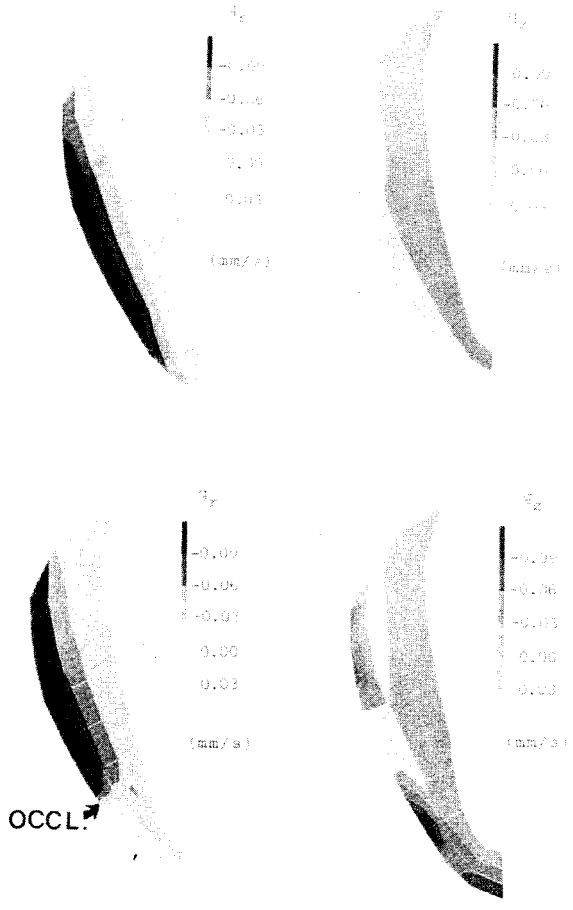

Fig. 9. Radial and axial coronary flow component in the basal situation (top) and after occlusion (bottom). The radial compartment is positive in the direction pointing away from the symmetry axis (on this picture: from right to left) and the axial component is positive from apex to base.

Conclusion

The finite element method opens new possibilities to the modelling of the coronary circulation. Although a great deal of uncertainty remains concerning the choice of the parameters, we can show that the model is able to reflect tendencies which are consistent with the experiment.

References

1. Streeter, D.D.Jr., Hanna, W.T., Engineering mechanics of successive states in canine left ventricular myocardium: II. Fiber angle and sarcomere length, Circ. Res. 33: 657-664, 1973.

2. Pinto, J.G., Fung, J.C., Mechanical properties of the heart muscle in the passive state, J. Biomechanics 6: 597-616, 1973.

3. Demer, L.L., Yin, F.C.P., Passive biaxial mechanical properties of isolated canine myocardium, J. Physiol. 339: 615-630, 1983.

4. Van Heuningen, R., Rijnsburger, W.H., ter Keurs, H.E.D.J., Sarcomere length control in striated muscle, Am. J. Physiol. 242, H411-420, 1982.

5. Westerhof, N., Elzinga, G., van den Bos, G.C., Influence of central and peripheral changes on the hydraulic input impedance of the systemic arterial tree, Med. Biol. Eng. 11: 710-722, 1973.

6. Arts, T., Veenstra, P.C., Reneman, R.S., Epicardial deformation and left ventricular wall mechanics during ejection in the dog, Am. J. Physiol. 243, H379-390, 1982.

7. Waldman, L.K., Fung, Y.C., Covell, J.W., Transmural myocardial deformation in the canine left ventricle: normal in vivo three-dimensional finite strains, Circ. Res. 57: 152-163, 1985.

8. Prinzen, f.W., Arts, T., van der Vusse, G.J., Reneman, R.S., Fiber shortening in the inner layers of the left ventricular wall as assessed from epicardial deformation during normoxia and ischemia, J. Biomech. 17: 801-811, 1984.

9. Heineman, F.W., Grayson, J., Transmural distribution of intramyocardial pressure measured by micropipette technique, Am. J. Physiol. 249: H1216-1223, 1985.

10. Spaan, F.A.E., Coronary diastolic pressure-flow relation and zero flow pressure explained on the basis of intramyocardial compliance, Circ. Res. 56: 293-309, 1985.